SPECTRAL ANALYSIS FOR BANDPASS NONLINEARITY WITH CYCLOSTATIONARY INPUT

Raviv Raich and G. Tong Zhou

School of Electrical and Computer Engineering, Georgia Institute of Technology, Atlanta, GA 30332-0250, USA

ABSTRACT

When a non-constant envelope signal goes through a nonlinear power amplifier, spectral regrowth (broadening) appears at the output of the power amplifier. To satisfy regulatory requirements on out of band emissions, spectral regrowth must be contained. In this paper, we derive a novel closed-form expression for the output power spectral density when the power amplifier is quasi-memoryless and cyclostationarity of the digitally modulated input is taken into account. We compare our results with the conventional analysis where stationary input is assumed. We emphasize the importance of paying attention to the cyclostationary nature of the input when excess bandwidth is present.

1. INTRODUCTION

Power amplifiers (PAs) are the major source of nonlinearity in communications systems. To achieve high efficiency from a given PA, the PA is sometimes driven into its nonlinear region. When a non-constant envelope signal goes through a nonlinear PA, spectral regrowth (broadening) appears at the PA output, which in turn causes adjacent channel interference (ACI). Due to stringent limits on the ACI imposed by regulatory bodies, PA nonlinearity must be limited.

It would be very helpful if we can predict spectral regrowth for a prescribed level of PA nonlinearity. Since more linear PAs are less efficient, practitioners may wish to use the PA in a configuration that allows for maximum PA efficiency while satisfying the spectral emission limits. Such an optimization strategy is feasible if we have tools for spectral analysis for the nonlinear device.

In the input is Gaussian and stationary, the PA output power spectral density (PSD) has been derived for a polynomial nonlinear PA model of any order in [1]. When the PA input is non-Gaussian, theoretical analysis becomes more complicated; however results are available in [2] for a 7th-order nonlinear PA with (non-)Gaussian inputs. In [3], phase randomization is used to “stationarize” a cyclostationary input. To the best of our knowledge, all spectral analysis results thus far assume the input to be stationary; see [1] for a literature review on spectral regrowth analysis.

In this paper, we offer an analytic approach to examine the stationarity of digitally modulated signals. Furthermore, we present novel spectral analysis results that take into account cyclostationarity of the input signal. A closed-form expression for the PA output spectrum will be given. We offer a comparison between the estimated PSD for the output of the PA, as well as analytic expressions for the PSD with and without the stationarity assumption. We show that when cyclostationarity of the input signal is taken into account, the PSD predicted by our formula matches well the PSD calculated from the data.

2. POWER AMPLIFIER MODELING

Consider the following baseband PA model [4, 5]:

$$y(t) = \sum_{k=0}^{K} a_{2k+1} |x(t)|^{2k} x(t), \tag{1}$$

where $x(t)$ is the baseband PA input signal, $y(t)$ is the baseband PA output signal, and $\{a_{2k+1}\}$ are complex-valued coefficients that can be extracted from standard characterizations (such as AM/AM, AM/PM curves) of the PA. The highest nonlinearity order is $2K+1$. The fact that only odd-order nonlinear terms appear in (1) is attributed to the bandpass nonlinear nature of the PA [4, 5].

We see from (1) that the PA complex gain is $G(x(t)) = y(t)/x(t) = \sum_{k=0}^{K} a_{2k+1}\ |x(t)|^{2k}$, which is a function of input amplitude $r = |x(t)|$ only. Writing the complex gain as $G(r) = A(r)\ e^{j\Phi(r)}$, we refer to $A(r)$ as the AM/AM conversion, and $\Phi(r)$ as the AM/PM conversion. A linear PA would have constant $A(r)$ and $\Phi(r)$ characteristics. If $A(r)$ is non-constant but $\Phi(r)$ is, the corresponding PA is called strictly memoryless. If both $A(r)$ and $\Phi(r)$ are non-constant, the resulting PA is called quasi-memoryless. Eq. (1) can be used to describe both types of memoryless nonlinearity, and hence we do not distinguish the two in subsequent analysis.

3. DIGITALLY-MODULATED SIGNALS

Consider the following baseband representation of a digitally-modulated signal:

$$x(t) = \sum_{k=-\infty}^{\infty} s_k h(t-kT), \tag{2}$$

where s_k is the kth symbol, $h(t)$ is impulse response of the pulse shaping filter, and T is the symbol period. Applying the continuous-time Fourier transform (CTFT) to both sides of (2), we obtain $X(f) = H(f)S(e^{j2\pi Tf})$, where the CTFT of $x(t)$ is defined as $X(f) = \mathcal{F}\{x(t)\} = \int x(t)e^{-j2\pi tf}dt$, the CTFT of $h(t)$ is $H(f) = \mathcal{F}\{h(t)\} = \int h(t)e^{-j2\pi tf}dt$, and the discrete-time Fourier transform (DTFT) of s_k is defined as $S(e^{j2\pi Tf}) = \sum_{k=-\infty}^{\infty} s_k e^{-j2\pi kTf}$. Note that $S(e^{j2\pi Tf})$ is periodic in f with period $\frac{1}{T}$, i.e., information contained in $f \in [-\frac{1}{2T}, \frac{1}{2T}]$ is repeated every $\frac{1}{T}$. To preserve the information in $S(e^{j2\pi Tf})$, the pulse shaping filter, $H(f)$, must have a bandwidth greater than or equal to $\frac{1}{T}$.

Assume that $\{s_k\}$ is zero-mean, i.i.d with variance $\gamma_{2s} = E[|s_k|^2]$. The mean and covariance function of $x(t)$ are re-

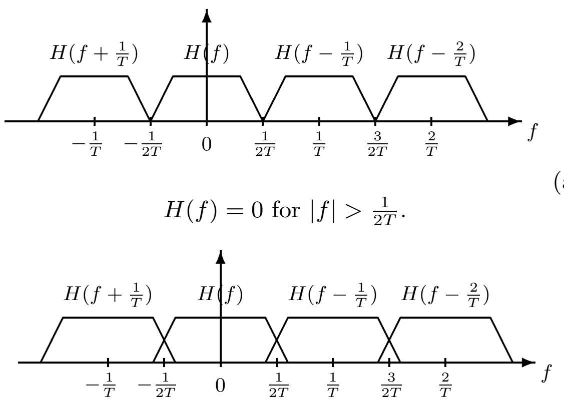

(a)

$H(f) = 0$ for $|f| > \frac{1}{2T}$.

(b)

$H(f) \neq 0$ for some $|f| > \frac{1}{2T}$.

Figure 1. Relationship among $H(f + \frac{m}{T})$.

spectively, $E[x(t)] = 0$,

$$\begin{aligned} c_{2x}(t;\tau) &= \mathrm{cum}\left\{x^*(t), x(t+\tau)\right\} \\ &= \gamma_{2s} \sum_{k=-\infty}^{\infty} h^*(t-kT)h(t+\tau-kT). \end{aligned} \quad (3)$$

Note that $x(t)$ is not wide-sense stationary (WSS) in general since (3) may depend on t.

In Appendix A, we show that $c_{2x}(t;\tau)$ can be separated into t-dependent terms and τ-dependent terms as follows:

$$c_{2x}(t;\tau) = \frac{\gamma_{2s}}{T} \sum_{m=-\infty}^{\infty} \rho_{\frac{m}{T}}(\tau) e^{-j\frac{2\pi}{T}mt}, \quad (4)$$

$$\rho_u(\tau) = \int H^*(f+u)H(f)e^{j2\pi f\tau}df. \quad (5)$$

Inverse CTFT is defined as $x(t) = \mathcal{F}^{-1}\{X(f)\} = \int X(f)e^{j2\pi ft}df$. From (5), we see that $\rho_u(\tau)$ and $H^*(f+u)H(f)$ form a CTFT pair. The time average of (4) is

$$c_{2x}(\tau) \triangleq \overline{c_{2x}(t;\tau)} = \frac{\gamma_{2s}}{T}\rho_0(\tau) = \frac{\gamma_{2s}}{T}\int |H(f)|^2 e^{j2\pi f\tau}df,$$

where $\overline{f(t)} \triangleq \lim_{\Delta\to\infty}\frac{1}{2\Delta}\int_{-\Delta}^{\Delta} f(t)dt$ represents the time averaging operation and $\rho_0(\tau) = \mathcal{F}^{-1}\left\{|H(f)|^2\right\}$.

With respect to $h(t)$, we consider the following two cases:
(i) **No excess bandwidth case.** When $H(f)$ is band-limited to bandwidth $\frac{1}{T}$, i.e., $H(f) = 0$ for $|f| > \frac{1}{2T}$, the only m for which $H(f + \frac{m}{T})$ overlaps with $H(f)$, is $m = 0$ (see Fig. 1(a)). In this case, $\rho_{\frac{m}{T}}(\tau) = 0$ except for $m = 0$. Therefore, the time-dependent term $e^{-j\frac{2\pi}{T}mt}$ in (4) is immaterial and $c_{2x}(t;\tau) = \frac{\gamma_{2s}}{T}\rho_0(\tau)$. Since $c_{2x}(t;\tau)$ does not depend on t, $c_{2x}(t;\tau) = c_{2x}(\tau)$ and $x(t)$ is WSS. If $x(t)$ is Gaussian (either real or complex) then it is also strict sense stationary (SSS).
(ii) **Excess bandwidth case.** When the bandwidth of $H(f)$ exceeds $\frac{1}{T}$ but does not exceed $\frac{2}{T}$, i.e., $H(f) \neq 0$ for some $|f| > \frac{1}{2T}$, but $H(f) = 0$ for $|f| > \frac{1}{T}$, the only m values for which $H(f+\frac{m}{T})$ overlaps with $H(f)$ are $m = 0$, $m = -1$, and $m = 1$ (see Fig. 1(b)). In this case, only $\rho_0(\tau)$, $\rho_{\frac{1}{T}}(\tau)$, and $\rho_{-\frac{1}{T}}(\tau)$ are non-zero, and hence from (4),

$$c_{2x}(t;\tau) = \frac{\gamma_{2s}}{T}\left(\rho_0(\tau) + \rho_{-\frac{1}{T}}(\tau)e^{j\frac{2\pi}{T}t} + \rho_{\frac{1}{T}}(\tau)e^{-j\frac{2\pi}{T}t}\right). \quad (6)$$

In this case $c_{2x}(t;\tau)$ is a function of both t and τ, meaning that $x(t)$ is not WSS.

4. CYCLOSTATIONARY SPECTRAL ANALYSIS

In the non-stationary case, the spectrum of the PA output is given by: $S_{2y}(f) = \mathcal{F}\{c_{2y}(\tau)\}$, where $c_{2y}(\tau)$ is the time-averaged version of $c_{2y}(t;\tau) = \mathrm{cum}\{y^*(t),\ y(t+\tau)\}$. We assume that the input $x(t)$ is Gaussian distributed, which is well-motivated for applications such as OFDM (orthogonal frequency division multiplexing). In [1], the auto-covariance function of $y(t)$ is obtained when $x(t)$ is a stationary complex-Gaussian random process. Generalizing the analysis in [1] to the non-stationary case yields:

$$\begin{aligned} c_{2y}(t;\tau) = \sum_{s=0}^{K} & \frac{1}{(s+1)}|c_{2x}(t;\tau)|^{2s} c_{2x}(t;\tau) \quad (7) \\ & \left(\sum_{l=s}^{K} a_{2l+1}\binom{l}{s}(l+1)!(c_{2x}(t;0))^{l-s}\right) \\ & \left(\sum_{k=s}^{K} a_{2k+1}\binom{k}{s}(k+1)!(c_{2x}(t+\tau;0))^{k-s}\right)^*, \end{aligned}$$

where $c_{2x}(t;\tau)$ is the auto-covariance of $x(t)$ and the input/output data model (1) is assumed. Note that in the stationary case, i.e., when $c_{2x}(t;\tau) = c_{2x}(\tau)$, equation (7) simplifies to:

$$\begin{aligned} c_{2y}(\tau) = \sum_{s=0}^{K} & \frac{1}{(s+1)}|c_{2x}(\tau)|^{2s} c_{2x}(\tau) \\ & \left|\sum_{l=s}^{K} a_{2l+1}\binom{l}{s}(l+1)!(c_{2x}(0))^{l-s}\right|^2, \quad (8) \end{aligned}$$

which is the result presented in [1] (see also [6]). In the cyclostationary case, we obtain the time average of (7) as

$$\begin{aligned} c_{2y}(\tau) = \sum_{s=0}^{K}\sum_{l=s}^{K}\sum_{k=s}^{K} & \frac{(l+1)!}{(s+1)}\binom{l}{s}(k+1)!\binom{k}{s}a_{2l+1} \quad (9) \\ a^*_{2k+1} & \overline{|c_{2x}(t;\tau)|^{2s}c_{2x}(t;\tau)(c_{2x}(t;0))^{l-s}(c^*_{2x}(t+\tau;0))^{k-s}}. \end{aligned}$$

Unfortunately, time-average of a product is not the same as the product of individual time-averages (e.g., $\overline{c_{2x}(t;\tau)c_{2x}(t,0)} \neq c_{2x}(\tau)c_{2x}(0)$) so (9) is not easily simplified.

For the digitally-modulated $x(t)$ of (2), we substitute (5) and (6) into (9) to obtain a closed-form expression for $c_{2y}(\tau)$ in terms of $H(f)$, γ_{2s}, and T. Its Fourier transform then yields the PSD $S_{2y}(f)$. For simplicity, we describe the result for a PA given by (1) with $K = 1$, i.e., including only the linear and cubic nonlinear terms. In this case, (9) becomes

$$\begin{aligned} c_{2y}(\tau) = |a_1|^2 & \underbrace{\overline{c_{2x}(t;\tau)}}_{①} + 2a_1a_3^* \underbrace{\overline{c_{2x}(t;\tau)c^*_{2x}(t+\tau;0)}}_{②} \quad (10) \\ +2a_1^*a_3 & \underbrace{\overline{c_{2x}(t;\tau)c_{2x}(t;0)}}_{③} + 4|a_3|^2 \underbrace{\overline{c_{2x}(t;\tau)c_{2x}(t;0)c^*_{2x}(t+\tau;0)}}_{④} \\ & + 2|a_3|^2 \underbrace{\overline{|c_{2x}(t;\tau)|^2 c_{2x}(t;\tau)}}_{⑤}. \end{aligned}$$

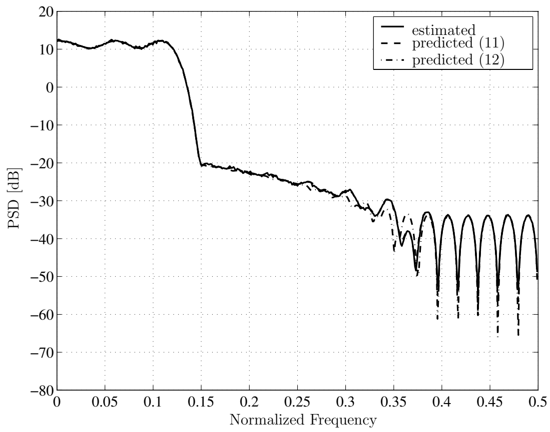

(a) with IS-95 pulse shaping filter.

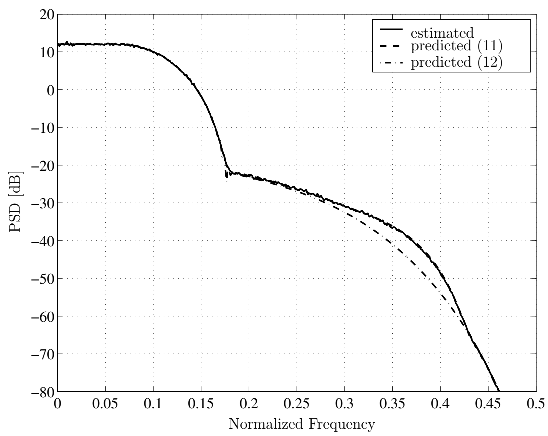

(b) with root raised cosine filter ($\beta = 0.5$).

Figure 2. PA output PSD for a third-order nonlinear PA. The solid line is the estimated PSD based on output samples; the dashed line corresponds to (11), and the dash-dotted line is generated using equation (12).

Substituting (6) into (10) and taking the CTFT on both sides of (10), we show in Appendix B that the PA output PSD is

$$\begin{aligned} S_{2y}(f) = \frac{\gamma_{2s}}{T}\Big|a_1 H(f) + a_3\frac{\gamma_{2s}}{T}\Big(\rho_0(0)H(f) \\ +\rho_{\frac{1}{T}}(0)H(f+\tfrac{1}{T}) + \rho_{-\frac{1}{T}}(0)H(f-\tfrac{1}{T})\Big)\Big|^2 \\ +2|a_3|^2(\frac{\gamma_{2s}}{T})^3\Big(|H(f)|^2 \star |H(f)|^2 \star |H(-f)|^2 \\ +2[H^*(f-\tfrac{1}{T})H(f)] \star [H(-f-\tfrac{1}{T})H^*(-f)] \star |H(f)|^2 \\ +2[H^*(f+\tfrac{1}{T})H(f)] \star [H(-f+\tfrac{1}{T})H^*(-f)] \star |H(f)|^2 \\ +2[H^*(f+\tfrac{1}{T})H(f)] \star [H^*(f-\tfrac{1}{T})H(f)] \star |H(-f)|^2\Big), \quad (11) \end{aligned}$$

where $\star$ denotes convolution. In the zero excess bandwidth (WSS) case, $H(f)$ and $H(f \pm \frac{1}{T})$ do not overlap, $H(f)H(f \pm \frac{1}{T}) = 0$, $\rho_{\frac{1}{T}}(0) = \rho_{-\frac{1}{T}}(0) = 0$, and thus (11) simplifies to

$$\begin{aligned} S_{2y}(f) = \frac{\gamma_{2s}}{T}\Big|a_1 + a_3\frac{\gamma_{2s}}{T}\rho_0(0)\Big|^2|H(f)|^2 \\ +2\left(\frac{\gamma_{2s}}{T}\right)^3|a_3|^2|H(f)|^2 \star |H(f)|^2 \star |H(-f)|^2. \quad (12) \end{aligned}$$

Next, we verify (11) and compare it with (12) using computer simulations.

5. NUMERICAL EXAMPLES

Consider the PA given in (1) with $K = 1$ and $a_1 = 15.0008 + 0.0908j$ and $a_3 = -23.0826 + 3.3133j$. Here, we explore the PA output PSD when the input $x(t)$ is given by (2) with the following pulse shaping filter (i) IS-95 pulse shaping filter [7], or (ii) root raised cosine filter given by $H(f) =$

$$\begin{cases} 1 & |f| < (1-\beta)f_c \\ \frac{1}{2} + \frac{1}{2}\cos\left(\pi\frac{f-(1-\beta)f_c}{2\beta f_c}\right) & (1-\beta)f_c \le |f| \le (1+\beta)f_c \\ 0 & |f| > (1+\beta)f_c \end{cases}$$

with cut-off frequency $f_c = \frac{1}{2T}$, and roll-off factor $\beta = 0.5$ (50% excess bandwidth). For both (i) and (ii), sampling rate is 4 samples per symbol. γ_{2s} is selected such that the variance of $x(t)$ is 0.017, and $|x(t)|$ enters into the compression region of the PA.

Figures 2(a) and 2(b) show the PA output PSD corresponding to filters (i) and (ii), respectively. The solid line is the PA output PSD obtained from 2^{17} samples of $y(t)$. The dashed line is the PA output PSD calculated based on (11). The dash-dotted line is the PA output PSD calculated based on (12) (i.e., assuming a stationary input data model). From both figures, we observe that the dashed line and the solid line coincide, thus verifying the theoretical expression in (11). The small gap (in the adjacent channel) between the solid line and the dashed-dotted line in Fig. 2(b) indicates that (12) cannot be used to accurately predict the PA output PSD when the input has excess bandwidth. Therefore, treating digitally-modulated signals with excess bandwidth as stationary underestimates out-of-band emission by as much as 6 dB for the example shown. For a different PA or a different input drive level, the discrepancy between stationary and nonstationary spectral analysis can be more or less than what we see here. The discrepancy is negligible in Fig. 2(a) because the filter has basically no excess bandwidth, except that small ripples are present outside the passband $[-\frac{1}{2T}, \frac{1}{2T}]$.

6. CONCLUSIONS

Power amplifiers are used in most communication systems and are inherently nonlinear. Spectral analysis can help to evaluate the suitability of a given PA for amplifying certain signals so the spectral mask of the intended application is met. In this paper, we investigated bandpass nonlinearities with Gaussian inputs. We took into account the cyclostationary nature of the digitally-modulated input. We showed that when the pulse shaping filter has no excess bandwidth, the input signal is WSS and previous results in [1] and [2] apply. We derived a novel closed-form expression for the PSD at the output of the PA when the input signal is cyclostationary which happens when the pulse shaping filter has excess bandwidth. We showed that spectral analysis assuming a stationary input does not accurately predict the PSD of the cyclostationary PA output, and the discrepancy can be resolved if cyclostationarity is taken into account.

A Derivation of Eq. (4)

The inverse CTFT of $H(f)$ is $h(t) = \int H(f)e^{j2\pi ft}df$. Substituting this into (3), we obtain

$$c_{2x}(t;\tau) = \gamma_{2s} \iint H^*(f_1)e^{-j2\pi f_1 t}H(f_2)e^{j2\pi f_2(t+\tau)} \sum_{k=-\infty}^{\infty} e^{j2\pi(f_1-f_2)kT}df_1 df_2. \quad (13)$$

Using the fact that $\sum_{k=-\infty}^{\infty} e^{j2\pi fkT}$ is the Fourier series expansion of $\sum_{m=-\infty}^{\infty} \frac{1}{T}\delta(f-\frac{m}{T})$, we rewrite (13) as

$$\begin{aligned} c_{2x}(t;\tau) &= \frac{\gamma_{2s}}{T}\sum_{m=-\infty}^{\infty}\int H^*(f_2+\frac{m}{T})e^{-j2\pi f_2 t} e^{-j\frac{2\pi}{T}mt}H(f_2)e^{j2\pi f_2(t+\tau)}df_2 \\ &= \frac{\gamma_{2s}}{T}\sum_{m=-\infty}^{\infty} e^{-j\frac{2\pi}{T}mt}\int H^*(f+\frac{m}{T})H(f)e^{j2\pi f\tau}df, \end{aligned}$$

which yields (4) and (5).

B Derivation of Eq. (11)

We substitute (6) into (10) and write out each of the time-averages. Recall that the time average of $e^{j\alpha t}$ is zero except when α is 0 modulo 2π.

$$① = \frac{\gamma_{2s}}{T}\rho_0(\tau) \quad (14)$$

$$② = \left(\frac{\gamma_{2s}}{T}\right)^2 \left(\rho_0(\tau)\rho_0^*(0) + \rho_{\frac{1}{T}}(\tau)\rho_{\frac{1}{T}}^*(0)e^{j\frac{2\pi}{T}\tau} + \rho_{-\frac{1}{T}}(\tau)\rho_{-\frac{1}{T}}^*(0)e^{-j\frac{2\pi}{T}\tau}\right) \quad (15)$$

$$③ = (\frac{\gamma_{2s}}{T})^2 \left(\rho_0(\tau)\rho_0(0) + \rho_{\frac{1}{T}}(\tau)\rho_{-\frac{1}{T}}(0) + \rho_{-\frac{1}{T}}(\tau)\rho_{\frac{1}{T}}(0)\right)$$

$$\begin{aligned} ④ = (\frac{\gamma_{2s}}{T})^3 \Big(&\rho_0(\tau)|\rho_0(0)|^2 + \rho_{\frac{1}{T}}(\tau)\rho_0(0)\rho_{\frac{1}{T}}^*(0)e^{j\frac{2\pi}{T}\tau} \\ &+\rho_{\frac{1}{T}}(\tau)\rho_{-\frac{1}{T}}(0)\rho_0^*(0) + \rho_0(\tau)|\rho_{\frac{1}{T}}(0)|^2 e^{j\frac{2\pi}{T}\tau} \\ &+\rho_0(\tau)|\rho_{-\frac{1}{T}}(0)|^2 e^{-j\frac{2\pi}{T}\tau} + \rho_{-\frac{1}{T}}(\tau)\rho_{\frac{1}{T}}(0)\rho_0^*(0) \\ &+\rho_{-\frac{1}{T}}(\tau)\rho_0(0)\rho_{-\frac{1}{T}}^*(0)e^{-j\frac{2\pi}{T}\tau}\Big) \end{aligned} \quad (16)$$

$$\begin{aligned} ⑤ = (\frac{\gamma_{2s}}{T})^3 \Big(&|\rho_0(\tau)|^2\rho_0(\tau) + 2|\rho_{-\frac{1}{T}}(\tau)|^2\rho_0(\tau) \\ &+2|\rho_{\frac{1}{T}}(\tau)|^2\rho_0(\tau) + 2\rho_{\frac{1}{T}}(\tau)\rho_{-\frac{1}{T}}(\tau)\rho_0^*(\tau)\Big). \end{aligned} \quad (17)$$

To obtain $S_{2y}(f)$, we take the CTFT of (10), i.e.,

$$\begin{aligned} S_{2y}(f) = \mathcal{F}\{c_{2y}(\tau)\} &= |a_1|^2\mathcal{F}\{①\} + 4\mathrm{Re}\,(a_1^* a_3 \mathcal{F}\{③\}) \\ &+4|a_3|^2\mathcal{F}\{④\} + 2|a_3|^2\mathcal{F}\{⑤\}. \end{aligned} \quad (18)$$

From (5), we see that the CTFT of $\rho_u(\tau)$ is $H^*(f+u)H(f)$. Therefore, the CTFT of (14)-(17) is respectively,

$$\mathcal{F}\{①\} = \frac{\gamma_{2s}}{T}|H(f)|^2 \quad (19)$$

$$\begin{aligned} \mathcal{F}\{②\} = (\frac{\gamma_{2s}}{T})^2\Big(&|H(f)|^2\rho_0^*(0) + \rho_{\frac{1}{T}}^*(0)H^*(f)H(f-\tfrac{1}{T}) \\ &+\rho_{-\frac{1}{T}}^*(0)\rho_{-\frac{1}{T}}(\tau)H^*(f)H(f+\tfrac{1}{T})\Big) \end{aligned} \quad (20)$$

$$\begin{aligned} \mathcal{F}\{③\} = (\frac{\gamma_{2s}}{T})^2\Big(&\rho_0(0)|H(f)|^2 + \rho_{-\frac{1}{T}}(0)H^*(f+\tfrac{1}{T})H(f) \\ &+\rho_{\frac{1}{T}}(0)H^*(f-\tfrac{1}{T})H(f)\Big) \end{aligned} \quad (21)$$

$$\begin{aligned} \mathcal{F}\{④\} = \ &(\frac{\gamma_{2s}}{T})^3\Big(|\rho_0(0)|^2|H(f)|^2 + \rho_0(0)\rho_{\frac{1}{T}}^*(0)H(f-\tfrac{1}{T})H^*(f) \\ &+\rho_{-\frac{1}{T}}(0)\rho_0^*(0)H^*(f+\tfrac{1}{T})H(f) + |\rho_{\frac{1}{T}}(0)|^2|H(f-\tfrac{1}{T})|^2 \\ &+|\rho_{-\frac{1}{T}}(0)|^2|H(f+\tfrac{1}{T})|^2 + \rho_{\frac{1}{T}}(0)\rho_0^*(0)H^*(f-\tfrac{1}{T})H(f) \\ &+\rho_0(0)\rho_{-\frac{1}{T}}^*(0)H(f+\tfrac{1}{T})H^*(f)\Big) \end{aligned} \quad (22)$$

$$\begin{aligned} \mathcal{F}\{⑤\} = (\frac{\gamma_{2s}}{T})^3\Big(&|H(f)|^2\star|H(f)|^2\star|H(-f)|^2 \\ &+2[H^*(f-\tfrac{1}{T})H(f)]\star[H(-f-\tfrac{1}{T})H^*(-f)]\star|H(f)|^2 \\ &+2[H^*(f+\tfrac{1}{T})H(f)]\star[H(-f+\tfrac{1}{T})H^*(-f)]\star|H(f)|^2 \\ &+2[H^*(f+\tfrac{1}{T})H(f)]\star[H^*(f-\tfrac{1}{T})H(f)]\star|H(-f)|^2\Big). \end{aligned} \quad (23)$$

Using the fact that $\rho_{\frac{1}{T}}(0) = \rho_{-\frac{1}{T}}^*(0)$, we simplify (21) as

$$\begin{aligned} \mathcal{F}\{③\} = (\frac{\gamma_{2s}}{T})^2 H(f)\Big(&\rho_0(0)H(f) + \rho_{\frac{1}{T}}(0)H(f+\tfrac{1}{T}) \\ &+\rho_{-\frac{1}{T}}(0)H(f-\tfrac{1}{T})\Big)^* \end{aligned} \quad (24)$$

and realize that $\mathcal{F}\{②\} = \mathcal{F}\{③\}^*$. Moreover, we use the fact that $H^*(f-\frac{1}{T})H(f+\frac{1}{T}) = 0$ to simplify (22) as

$$\mathcal{F}\{④\} = (\frac{\gamma_{2s}}{T})^3\Big|\rho_0(0)H(f) + \rho_{-\frac{1}{T}}(0)H(f-\tfrac{1}{T}) + \rho_{\frac{1}{T}}(0)H(f+\tfrac{1}{T})\Big|^2. \quad (25)$$

Substituting (19), (24)-(25) and (23) back into (18), we obtain (11).

REFERENCES

[1] G. T. Zhou and R. Raich, "Spectral analysis of polynomial nonlinearity with applications to RF power amplifiers." submitted to EURASIP Journal on Applied Signal Processing, special issue on nonlinear signal and image processing, Sep. 2003. See also *Proc. IEEE - EURASIP Workshop on Nonlinear Signal and Image Processing*, (Grado, Italy), June 2003.

[2] G. T. Zhou and J. S. Kenney, "Predicting spectral regrowth of nonlinear power amplifiers," *IEEE Trans. on Communications*, vol. 50, pp. 718–722, May 2002.

[3] V. Aparin and L. E. Larson, "Analysis and reduction of cross-modulation distortion in CDMA receivers," *IEEE Trans. Microwave Theory and Techniques*, vol. 51, pp. 1591–1602, May 2003.

[4] S. Benedetto, E. Biglieri, and R. Daffara, "Modeling and performance evaluation of nonlinear satellite links — a Volterra series approach," *IEEE Trans. on Aerospace and Electronic Systems*, vol. 15, pp. 494–507, July 1979.

[5] S. Benedetto and E. Biglieri, *Principles of Digital Transmission With Wireless Applications*. Kluwer Academic Publishers, July 1999.

[6] N. Blachman, "The output signals and noise from a nonlinearity with amplitude-dependent phase shift," *IEEE Trans. Inform. Theory*, vol. 25, pp. 77–79, Jan. 1979.

[7] TIA/EIA-95. *Mobile Station - Base Station Compatibility Standard for Dual-Mode Wideband Spread Spectrum Cellular Systems*, TIA, 1997.